Atmospheric Environment 109 (2015) 23–30

Contents lists available at ScienceDirect

Atmospheric Environment

journal homepage: www.elsevier.com/locate/atmosenv

Long-range transport of air pollutants originating in China: A possible major cause of multi-day high-PM_{10} episodes during cold season in Seoul, Korea

Hye-Ryun Oh [a], Chang-Hoi Ho [a, *], Jinwon Kim [b], Deliang Chen [c], Seungmin Lee [a], Yong-Sang Choi [d], Lim-Seok Chang [e], Chang-Keun Song [e]

[a] School of Earth and Environmental Sciences, Seoul National University, Seoul, Republic of Korea
[b] Department of Atmospheric and Oceanic Sciences, UCLA, Los Angeles, CA, USA
[c] Department of Earth Sciences, University of Gothenburg, Gothenburg, Sweden
[d] Department of Environmental Science and Engineering, Ewha Womans University, Seoul, Republic of Korea
[e] Air Quality Research Division, National Institute of Environment Research, Incheon, Republic of Korea

HIGHLIGHTS

- We examined a possible cause of the onset of multi-day high-PM_{10} episodes in Seoul.
- The episodes mainly occur by a strong high-pressure and weak westerlies.
- The atmospheric fields help trans-boundary pollutant transports from China to Seoul.

ARTICLE INFO

Article history:
Received 30 October 2014
Received in revised form
28 February 2015
Accepted 4 March 2015
Available online 5 March 2015

Keywords:
PM_{10} episode
Long-lasting
Trans-boundary transport
Seoul
China

ABSTRACT

Massive air pollutants originating in China and their trans-boundary transports are an international concern in East Asia. Despite its importance, details in the trans-boundary transport of air pollutants over East Asia and its impact on regional air quality remain to be clarified. This study presents an evidence which strong support that aerosols emitting in China play a major role in the occurrence of multi-day (≥4 days) severe air pollution episodes in cold seasons (October through March) for 2001–2013 in Seoul, Korea, where the concentration of PM_{10} (particulates with diameters ≤ 10 μm) exceeds 100 μg m^{-3}. Observations show that these multi-day severe air pollution episodes occur when a strong high-pressure system resides over the eastern China–Korea region. In such weather conditions, air pollutants emitted in eastern China/southwestern Manchuria are trapped within the atmospheric boundary layer, and gradually spread into neighboring countries by weak lower tropospheric westerlies. Understanding of trans-boundary transports of air pollutants will advance the predictability of local air quality, and will encourage the development of international measures to improve air quality.

1. Introduction

Rapid industrialization and urbanization have seriously degraded air quality (Yasunari et al., 2013; Fajersztajn et al., 2013) in many regions around the world, particularly in China where explosive growths in industrial activities have occurred over recent decades. Exposure to high levels of air pollutants has become a serious public health hazard and is causing an increase in cardiac and respiratory morbidity and mortality (Brook et al., 2004; Chen and Kan, 2008; Fajersztajn et al., 2013). Air pollution was ranked as the ninth highest risk factor for the global burden of disease, and is expected to be the most serious environmental cause of premature deaths by 2050 (OECD, 2012; Gold and Samet, 2013). Recognizing such serious health effects, the World Health Organization (WHO) has introduced a guideline that the concentration of inhalable PM_{10} (particulates with diameters ≤ 10 μm) must not exceed 20 μg m^{-3} and 50 μg m^{-3} for the annual- and 24-h averages, respectively (WHO, 2005). However, the annual-mean PM_{10} level in

* Corresponding author.
E-mail address: hoch@cpl.snu.ac.kr (C.-H. Ho).

http://dx.doi.org/10.1016/j.atmosenv.2015.03.005

major cities in the Middle East, India, and in South-East Asia currently well exceeds 100 μg m^{-3} (WMO/IGAC, 2012).

In China, the annual-mean PM_{10} concentration decreased slightly from 120 μg m^{-3} in 2003 to 100 μg m^{-3} in 2009, but not for winter seasons due to the increase in coal combustion for heating (Zhang et al., 2007; Zhu et al., 2011; Liu et al., 2014). Particularly, since the anthropogenic PM occurred in cold seasons contains massive amounts of harmful substances such as toxic and heavy metal (e.g., So_2, NO_x, Pb, As, Ni, and etc.), the impact of these particles on health is extremely serious (Liu et al., 2014.; Zhang et al., 2014). In 2003, approximately 350,000–400,000 premature deaths in China were attributed to air pollution, and the economic burden of premature mortality and morbidity was estimated at 157 billion Chinese yuan (Shen et al., 2014). However, socio-economic losses and air quality problems due to the emissions in China are not confined to China because these air pollutants also affect the region immediately downwind from the major source region in China including Korea and Japan, and sometimes as far downstream as the western North American region across the Pacific Ocean (Heo et al., 2009; Fu et al., 2014; Lin et al., 2014). For instance, on January 12, 2013, the hourly averaged PM concentration in urban areas of central and eastern China were over 700 μg m^{-3}, with the extremes levels reaching up to 900 μg m^{-3} and continuing for approximately one week (Park et al., 2013; Wang et al., 2014). During the period, Seoul (the capital and the largest city in Korea) experienced four consecutive days with the PM_{10} level $\geq$ 100 μg m^{-3} (January 12–15, 2013), which resulted in an abnormally large number of respiratory admissions and caused traffic congestion and flight cancellations (Park et al., 2013).

It is strongly suspected that large amounts of air pollutants emitted in China are directly related to high-PM_{10} episodes in Seoul, a metropolitan area of a large population (the densest region of the OECD in Asia in 2012, and the second densest worldwide after Paris) which is in the immediately outflow region from the major source regions in China (OECD, 2013). Several short-term studies have shown evidences that air pollutants emitted in China reach its neighbors cross their border using data from international field experiments such an ACE-ASIA, ABC-EAREX, and remote sensing (Nakajima et al., 2007; Lee et al., 2013; Lewandowska and Falkowska, 2013; Wang et al., 2014). However, the effect of trans-boundary air pollutant transports on the long-term (multiple days) air quality in Seoul have not been analyzed. In addition, only few studies have examined possible causes of the occurrence of high-PM_{10} episodes for various periods, from one day to several days.

This study examines the atmospheric circulations and resulting trans-boundary pollutant transports associated with multi-day ($\geq$4-day) high-PM_{10} concentration episodes in Seoul during cold seasons (October through March) in the recent 13-year period, 2001–2013. To examine the processes behind the multi-day high-PM_{10} episodes and its link with air pollutants originating in China, we analyze meteorological fields (e.g., geopotential height and 3-D wind) that are directly related with the horizontal and vertical transport of air pollutants in East Asia. Further, to examine if the mechanism can be generalized for most of the high-PM_{10} episodes in Seoul, we compare the meteorological conditions in short-lasting (1-day) cases vs. multi-day cases. Analyses of meteorological conditions are then augmented by analyses of surface PM_{10} observations in China, back trajectory analysis, and the aerosol vertical profiles retrieved from the Cloud-Aerosol Lidar with Orthogonal Polarization (CALIOP). This study reveals that multi-day high-PM_{10} episodes in Seoul are directly linked with long-range low-tropospheric transport of air pollutants originating in north-eastern China.

2. Data and method

We have analyzed the hourly PM_{10} mass concentration data during the cold season of 2001–2013 at 27 air quality monitoring stations in Seoul. To minimize the local effect, the stations affected by the emissions from local vehicles and industrial plants (e.g., that show high PM_{10} fluctuations over a day/week) were excluded from this study. The PM_{10} concentration at these stations is measured by the increase in attenuation when beta rays irradiate particulate matter collected on a filter, the beta-ray absorption method (Chang and Tsai, 2003). The bias in this method is known to be about 10%, mainly due to particle-containing moisture (Chang and Tsai, 2003; Jung et al., 2007). The recorded hourly data is used to obtain the daily average values.

To examine the potential source of air pollutants and their trans-boundary transports, daily meteorological data such as geopotential height and the 3-D wind in Seoul was obtained from the National Centers for Environmental Prediction-National Center for Atmospheric Research (NCEP-NCAR) reanalysis 2. The data have a horizontal resolution of 2.5° × 2.5° longitude–latitude, and in the vertical data are distributed on 17 levels of pressure (Kalnay et al., 1996).

We further analyzed the PM_{10} concentration in China and 72-h back trajectories from Seoul to examine the possible paths of air pollutants from upstream regions. Since 2000, China has reported a daily averaged air pollution index (API) in terms of air quality monitoring in many cities (Zhang et al., 2003; Qu et al., 2010). A value for the API can be converted to a mass concentration of PM_{10} using the following equation:

$$PM_{10} = \left[\frac{API - API_{low}}{API_{high} - API_{low}}\right] \times \left(PM_{10\ high} - PM_{10\ low}\right) + PM_{10\ low}.$$

API_{high} and API_{low} are the upper and lower standard indices, respectively, and $PM_{10\ high}$ and $PM_{10\ low}$ are the PM_{10} mass concentrations corresponding to API_{high} and API_{low}, respectively. The upper and lower limits of the API and detailed calculation of PM_{10} concentration are in Zhang et al. (2003) and Qu et al. (2010). The uncertainty in daily PM_{10} measurements is less than 1% (Zhang et al., 2003). This study utilizes PM_{10} concentrations converted from the API at 83 stations in China for January 2001–March 2012.

We used CALIOP level-2 vertical feature mask data, with horizontal and vertical resolutions of 333 m and 30 m below 8.2 km, and 1000 m and 60 m from 8.2 km to 20.2 km, respectively (Omar et al., 2009; Winker et al., 2013). Since the data are only available after April 2006, we analyzed the vertical aerosol profiles for every high-PM_{10} episode from May 2006–December 2013. Aerosol in CALIOP is retrieved by the Cloud Aerosol Discrimination (CAD) algorithm: the probability distribution functions of the altitude-and-latitude-dependent feature integrated color ratio, layer-integrated volume depolarization ratio, and attenuated backscatter coefficient in 532 nm. Accordingly, a CAD score between −100 (0) and 0 (100) denotes aerosol (cloud), which is used to give the confidence level. Thus, we only used aerosol pixels with a medium ($50 \leq |\text{CAD score}| < 70$) or high ($|\text{CAD score}| \geq 70$) confidence score to minimize the effect of misclassification between aerosol and cloud.

A NOAA Hybrid single-particle Lagrangian integrated trajectory (HYSPLIT) model was employed to calculate air mass back trajectories (http://www.arl.noaa.gov/ready/hysplit4.html) (Draxler and Rolph, 2013). The meteorology of the archived NCEP-NCAR datasets (e.g., temperature, surface pressure, geopotential height, and 3-D wind) was used as the input for calculating the transport of air parcels. The 72-h backward trajectory of each high-PM_{10} episode in Seoul for 2001–2013 was performed with a 1-h time interval for three levels (e.g., 500, 1000, and 2000 m) above the ground level.

3. High-PM_{10} days in Seoul during the cold seasons of 2001–2013

Based on the criteria for PM_{10} concentration specified in the environmental protection law of the Republic of Korea, high-PM_{10} episodes are defined in this study using the daily-mean PM_{10} threshold value of 100 μg m^{-3}. To distinguish the high-PM_{10} episodes caused by the anthropogenic emissions from those caused by the natural phenomena such as Asian dust storms, yellow dust days (67 days in the 13-year period) issued by the Korea Meteorological Administration (http://web.kma.go.kr/eng/weather/asiandust/intro.jsp), were excluded in this analysis. A total of 215 days of high-PM_{10} episodes in the analysis period that meet these criteria were selected for further analysis. Among 215 high-PM_{10} days, 172 days (80%) are in extended episodes that lasted for two to seven consecutive days, and 76 days (35%) are in episodes that lasted for four or more consecutive days (i.e., multi-day in this study). The daily average PM_{10} concentration in these multi-day episodes exceeds 135.5 μg m^{-3}, nearly seven times the level (i.e., 20 μg m^{-3}) specified by WHO.

Differences in key specifics (such as emission sources and atmospheric transport) between the multi-day and 1-day high-PM_{10} episodes are examined below. Fig. 1 shows the annual- (○) and cold season- (●) averaged PM_{10} concentrations, and high-PM_{10} days included in the multi-day (filled bars) and 1-day (open bar) episodes during the cold seasons of 2001–2013. In general, the cold-season PM_{10} concentrations exceed the annul-mean values except for 2005. The cold season- (annual-) mean PM_{10} concentration decreases noticeably over the analysis period, from 83.7 (77.5) μg m^{-3} in 2002 to 45.5 (41.1) μg m^{-3} in 2012. Accordingly, the total number of high-PM_{10} days (combined 1-day and multi-day

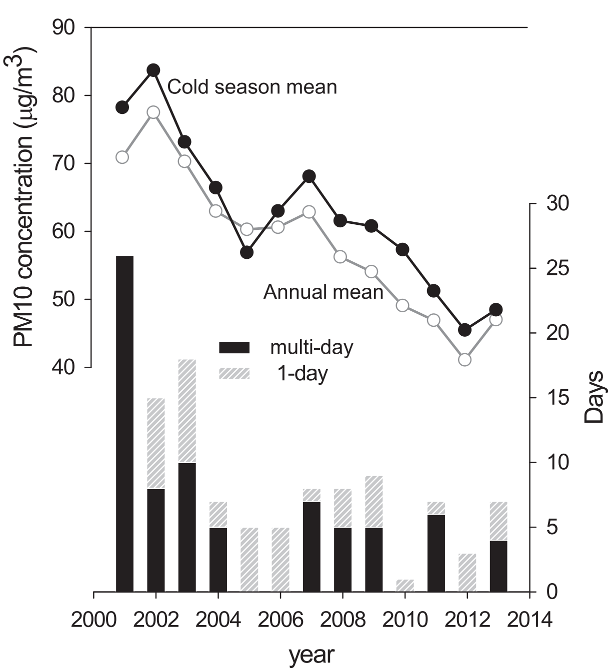

Fig. 1. Annually averaged (○) and cold season averaged (●) PM_{10} concentration, days of high-PM_{10} concentration episodes (≥100 μg m^{-3} day^{-1}) from 27 air quality monitoring stations in Seoul. Black and gray bars denote the multi-day (≥4 days) and 1-day episodes in cold season of each year, respectively.

episodes; the total bar lengths in Fig. 1) has also decreased over the 13-year period. However, the annual-mean number of deaths and inpatient admissions due to respiratory problems have remained at the same level for the 13 year period (data available from Korean Statistical Information Service, http://kosis.kr/). In addition, the number of high-PM_{10} days included in multi-day episodes remains similar from 2004 to 2013. Except for 2001, multi-day high-PM_{10} episodes have occurred one or two times per year regardless of annual-mean PM_{10} levels, which amounts to approximately four to ten days in total. In unusual case of 2001, the multi-day episode was frequent (13 days) in late October and November because of relatively high PM_{10} level in China (Wang et al., 2012), and recurrent long lasting fog and haze over Seoul region.

Here, we ask a question "why multi-day episodes has not decreased?" External factors in addition to local emissions in the Seoul metropolitan area, may also be responsible to the occurrence of multi-day high-PM_{10} episodes. Note that previous studies (e.g., Lee et al., 2011) found that the prevailing northwesterly wind in the cold season is favorable for long-range transportation of air pollutants from China into Korea. Thus, analyses of atmospheric circulation characteristics (Chen et al., 2008; Wang et al., 2010), particularly the pressure and wind distributions that affect the transport, dispersion, and accumulation of PM_{10} during the high-PM_{10} episodes, are essential for understanding the processes behind these multi-day high-PM_{10} episodes including the origins of the pollutants, in the Seoul metropolitan area.

4. Trans-boundary transport of PM_{10} from China to Seoul: atmospheric circulation analysis

To identify the atmospheric conditions favorable for transporting air pollutants from the major source regions in China to Seoul during the multi-day high-PM_{10} episodes, we analyzed the large-scale atmospheric circulation on the pressure-longitudinal cross section along the latitude of 37.7°N that crosses Seoul on the onset dates of multi- or 1-day episodes (Fig. 2). To remove seasonality, monthly climatology has been removed from these atmospheric fields before analyses.

Fig. 2 depicts the composites of anomalous geopotential height (a and e), pressure vertical velocity (b and f), zonal wind (c and g), and meridional wind (d and h) for the multi-day and 1-day episodes. Overall patterns are similar for these two types of episodes. As noted in previous studies (Chen et al., 2008; Lee et al., 2011), both types fulfill atmospheric conditions that are favorable for high-PM_{10} episodes in Seoul: High pressure anomalies and relatively weak winds near the surface. However, regional variations in magnitudes and features differ considerably from each other. For the multi-day episodes, high pressure anomalies extend from the surface to the upper troposphere (Fig. 2a) across the eastern China–Korea region against strong low pressure anomalies over western North Pacific. The high pressure system results in a general sinking motion (see the positive pressure velocity shown in Fig. 2b) which is favorable for high-PM_{10} concentrations near the surface as air pollutants are trapped and transported from high levels into the boundary layer. For the 1-day episodes, the high pressure anomaly over the China–Seoul region tilts vertically with relatively weak intensity in the low level below 700 hPa. As a consequence, the weak anomalous high-pressure near the surface and a low pressure anomaly below 800 hPa over eastern China (Fig. 2e) lead to a vertically stretched rising motion over China and Seoul (Fig. 2f). Thus, massive amounts of air pollutants emitted from the heavily urbanized and industrialized areas in eastern China can be transported above the boundary layer over Seoul. As a result, the transport of air pollutants within the boundary layer is weak for the

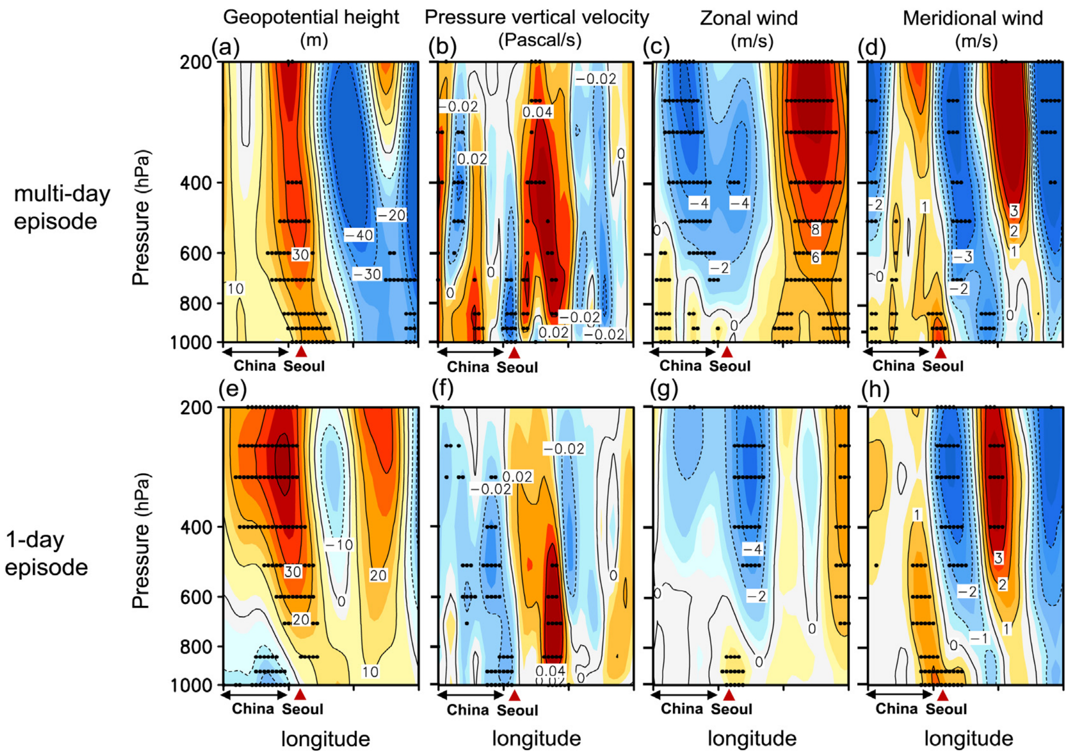

Fig. 2. Composite of anomalous geopotential height (a and e), pressure vertical velocity (b and f), zonal wind (c and g), and meridional wind (d and h) at 37.5°N as functions of longitude and pressure on the onset day of multi-day (upper panel) and 1-day (lower panel) high-PM_{10} concentration episodes. To remove seasonality of these atmospheric fields, the anomaly values against monthly climatology have been calculated. Block dots denote the regions significant at the 90% confidence level based on a *t*-test.

atmospheric conditions corresponding to 1-day episodes.

We also identified the difference in the zonal wind field between the two episode types. Fig. 2c shows a distinct decrease in the westerly above the 800 hPa level over China, Korea, and the neighboring western Pacific, implying anomalously stagnant conditions in the lower troposphere for the multi-day episodes. In contrast, Fig. 2g shows that anomalously positive westerlies occur around Seoul between the surface and up to the 600 hPa level, indicating dispersion of air pollutants over a deep layer (about 4 km thick) in the lower troposphere. The general features of the meridional wind are similar for the two types of episodes: southerly and northerly over the left and right of 135°E, respectively (Fig. 2d and h).

Fig. 3 shows the horizontal distribution of the geopotential height and wind field anomalies. Intensity of the anomalous high pressure system is clearly distinguishable between these two episode types. For the multi-day episode, both the Korean Peninsula and eastern China are highly affected by anomalous high pressure (Fig. 3a and b). Meanwhile, for the 1-day episode, the Korean Peninsula is seen to be affected by the rim of a high pressure anomaly with a center located near Japan, whereas eastern China is located under a low pressure anomaly (Fig. 3c and d). Thus, the westerlies (southerlies) are more dominant for multi-day (1-day) episodes (Fig. 3a and c, respectively), indicating that the atmospheric circulation during the multi-day episodes is more favorable for transporting pollutants from eastern China into Seoul than that occurring during 1-day episodes. In addition, for multi-day episodes, a strong low anomaly over northern Mongolia and western Pacific will play a major role in blocking the migratory anticyclone (Fig. 3a and b).

It is noteworthy that atmospheric circulations over the eastern China–Korea region appear two days before the onset of a multi-day episode (Fig. 4). Such circulations include strong and widespread high pressure anomalies located in the lower troposphere over the entire region of China (Fig. 4a and b) that are favorable for the occurrence of high-PM_{10} levels in central and eastern China by trapping air pollutants within the boundary layer. Additionally, a strong low pressure anomaly over the East Sea and the Okhotsk Sea to the east of the Korean Peninsula further help conditions favorable for multi-day high-PM_{10} episodes by blocking. Those indicate that the impact of air pollutants originating in China can be intensified under a favorable atmospheric circulation condition. By comparison, for 1-day episode both the size and intensity of high- (low-) pressure anomaly over China (East Sea) are relatively small and weak, respectively (Fig. 4c and d). This means that pollutants emitted in the surface level may easily be transported into upper layers and eastward.

Through an analysis of the atmospheric fields above, we have identified the pressure and wind patterns that are more favorable for multi-day episode occurrences, and which can be considered as the pathways for moving air pollutants. In multi-day episodes, PM_{10} is slowly transported in the lower troposphere from China to Seoul, while in the 1-day episodes ascending pollutants from eastern China are first transported via in relatively higher altitudes into the Seoul area. The following section presents the surface and satellite data that support the evidence obtained in this analyses of atmospheric fields.

5. Analyses of surface and satellite observations

To further clarify the results from the atmospheric field analysis for the two types of high-PM_{10} episodes discussed above, we examined the API in China, the back trajectory, and the CALIOP satellite-observed aerosol vertical profiles (Figs. 5 and 6). It is notable that the relatively strong and large anomalous high across China and Seoul is favorable for the accumulation of air pollutants

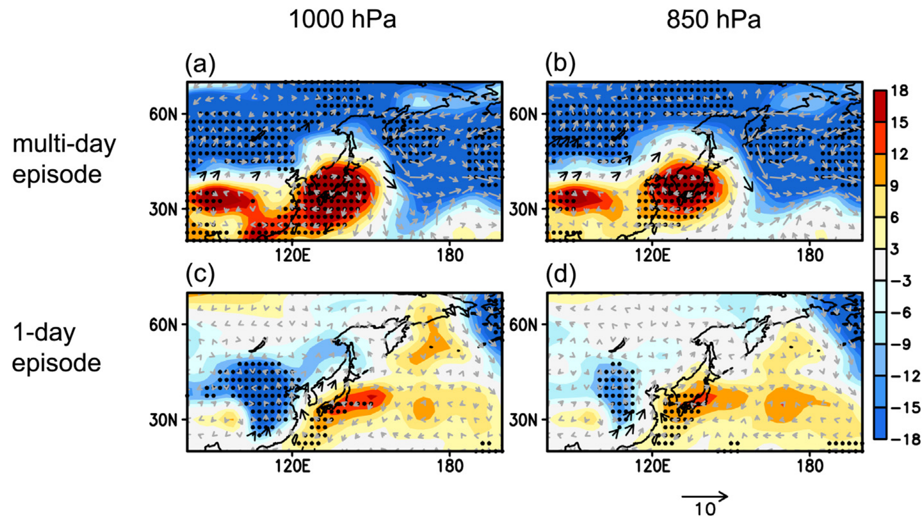

Fig. 3. Composite of anomalous geopotential height and wind vector at 1000 hPa (a and c) and 850 hPa (b and d) on the onset day of multi-day (upper panel) and 1-day (lower panel) high-PM_{10} concentration episodes. To remove seasonality of these atmospheric fields, the anomaly values against monthly climatology have been calculated. Black dots denote the regions significant at the 90% confidence level based on a *t*-test.

in the lower troposphere, and thus for multi-day high-PM_{10} episodes.

We analyzed the regional distribution of PM_{10} concentration anomalies at 83 stations in China in two and three days prior to both types of high-PM_{10} episodes in Seoul (Fig. 5). For both episode types, positive PM_{10} anomalies are found at most stations in central and southern China (where anomalous high pressure occur in). The positive anomalies are much larger for multi-day episodes than for 1-day episodes. In northeast China, the feature is generally opposite; positive PM_{10} concentration anomalies are dominant in multi-day episodes in contrast to the negative PM_{10} concentration anomalies in 1-day episodes. Among the 83 stations, the PM_{10} levels in north- and mid-eastern China (e.g., Shenyang, Beijing, Tianjin, and Shanghai) are relatively high, indicating potential source regions of the multi-day high-PM_{10} episode (Fig. 5a and b). In particular, anomalously high-PM_{10} levels over these regions occurring two and three days prior to an episode is perhaps due to the increased use of heating fuel during anomalously cold periods. In most stations, PM_{10} concentration gradually increases from three days to a day before the onset of both episode types. Consequently, in large areas of central and eastern China, the PM_{10} concentration one day prior to a multi-day high-PM_{10} onset in Seoul is 80–160 μg m^{-3} higher than the normal concentration of the same period (Fig. 6a). The area-mean PM_{10} concentrations for multi-day and 1-day episodes are 239.9 μg m^{-3} and 175.9 μg m^{-3}, respectively. A maximum PM_{10} level occurring one day before the beginning of an episode in Seoul reflects the accumulation of pollutants by a high-pressure system. This therefore implies that for multi-day episodes, relatively large amounts of pollutants can be transported from China into the Seoul area.

In order to identify the aerosol pathways during the high-PM_{10} episodes in Seoul, we performed backward trajectory calculations using the NOAA HYSPLIT model at 500, 1000, and 2000 m altitudes over a 72-hr period from the onset of each high-PM_{10} episode in Seoul. Fig. 6a and b (6d and 6e) show the mean horizontal and vertical pathways for the multi-day (1-day) episodes. The trajectory is significantly shorter for multi-day episodes than for 1-day episodes, indicating relatively stagnant low troposphere, which is consistent with the very weak zonal wind field shown in Fig. 2c. The horizontal and vertical transport routes also vary according to

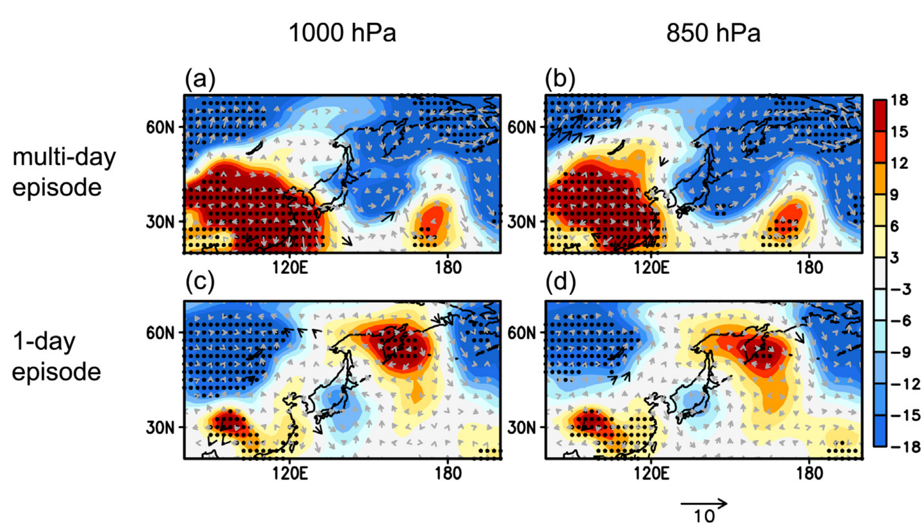

Fig. 4. Same as Fig. 3, except for −2 day high-PM_{10} concentration episodes.

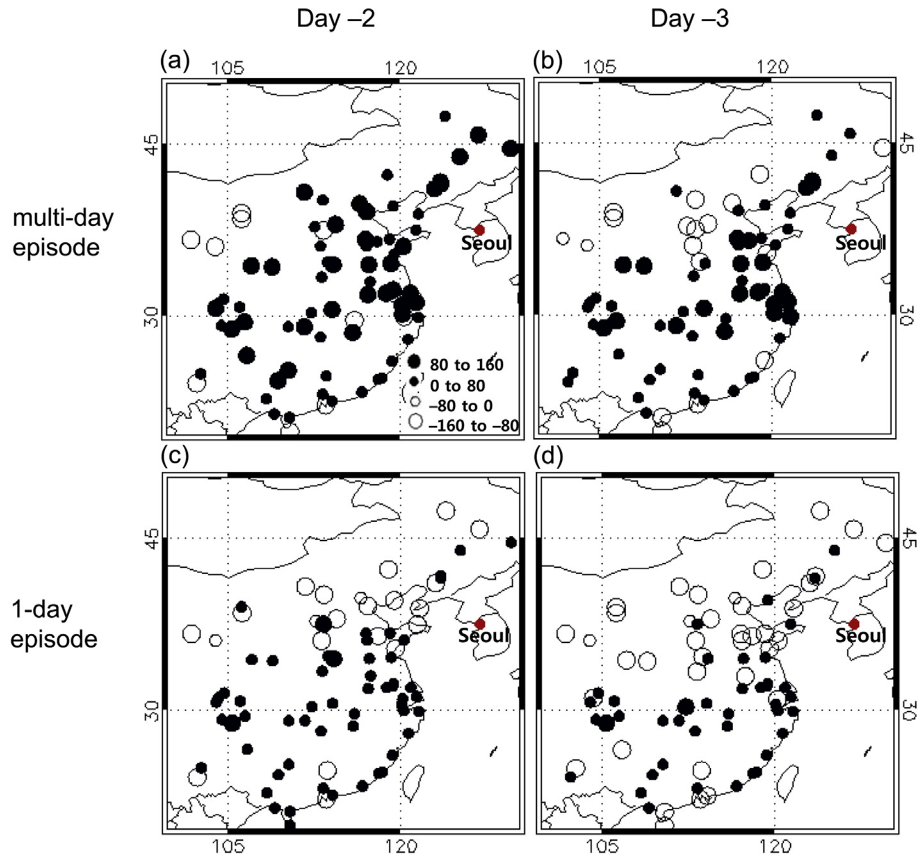

Fig. 5. Spatial distribution of anomalous PM_{10} concentrations measured from each of the 83 sites on −2 day and −3 day of multi-day (a and b) and 1-day (c and d) high-PM_{10} episodes.

the episode types. Among the heavily polluted regions (e.g., Shenyang, Beijing, Tianjin, and Shanghai) in China, the mean airflow passes through Beijing and Tianjin in multi-day episodes (Fig. 6a), but not in 1-day episodes (Fig. 6d). This means that air pollutants from Beijing and Tianjin may affect the occurrence of multi-day high-PM_{10} episode in Seoul. In addition, on the −2 day of (i.e., two days prior to) a multi-day episode, northwesterlies are dominant in the lower troposphere along the east rim of the anticyclone located over China (Fig. 4a and b). As the anticyclone moves toward Korea on the 0 day of an episode (Fig. 3), these pressure and wind may continuously maintain the supply from China and the accumulation of air pollutants in Seoul. Further, from −1 day of a multi-day episode, the low tropospheric air flow paths are nearly horizontal from the Yellow Sea to the Seoul area, while they slant down from relatively higher levels in 1-day episodes (Fig. 6b and e).

The difference in transport patterns may result in disparities in the aerosol vertical profiles between the two types of episodes in Seoul and its vicinity. We further examined the aerosol profiles using the CALIOP vertical feature mask. However, because the data are only available after April 2006, we looked at five and 19 onset days for multi-day and 1-day episodes, respectively. To extract aerosols over Seoul and its immediate neighboring areas, we only employed the CALIOP track data within ±1.5° from Seoul, both in latitude and longitude. Applying these criteria, two and seven collocated CALIOP tracks were identified for multi-day and 1-day episodes, respectively, after April 2006. Although this analysis was limited by the small number of samples, it is beneficial to examine the vertical distribution of aerosols as this can provide independent and additional evidence related to the link between aerosol sources in East Asia, trans-boundary transport, and pollutant concentration in Seoul. Fig. 6c and f shows the aerosol pixel numbers for each level in each collocated case for multi-day and 1-day episodes, respectively. There is a substantial difference in the vertical profiles between these two episode types. Unlike in 1-day episodes where notable aerosol concentrations occur throughout the troposphere up to the 10 km level (Fig. 6f), most aerosols are confined below the 1 km level in multi-day episodes (Fig. 6c) which is closely related to the low-level accumulation of aerosols under stable atmospheric conditions associated with a high-pressure system (Fig. 2a). This finding is also consistent with the back trajectory analysis results (Fig. 6a and b); pollutants during multi-day episodes are mostly spread within the boundary layer from the severely polluted regions in northeastern China. Aerosol profiles on extended high-PM_{10} episodes show high aerosol concentrations in the boundary layer. In conjunction with low-level winds (Figs. 2 and 3), this suggests strong aerosol transport from northeastern China into Seoul. The situation is very different for 1-day episodes; the aerosol concentration in the low troposphere is much lower than for multi-day episodes: 1-day episodes are mainly caused by local emissions.

6. Summary and discussion

We examined the atmospheric circulations and trans-boundary pollutant transports during multi-day (≥4-day) high-PM_{10} concentration episodes in Seoul in the cold season. The meteorological conditions over East Asia on the onset days of each episode type, the trajectories arriving at Seoul during episodes, and the horizontal and vertical distributions of aerosols over China and Korea before and after high PM_{10} episodes strongly imply that the

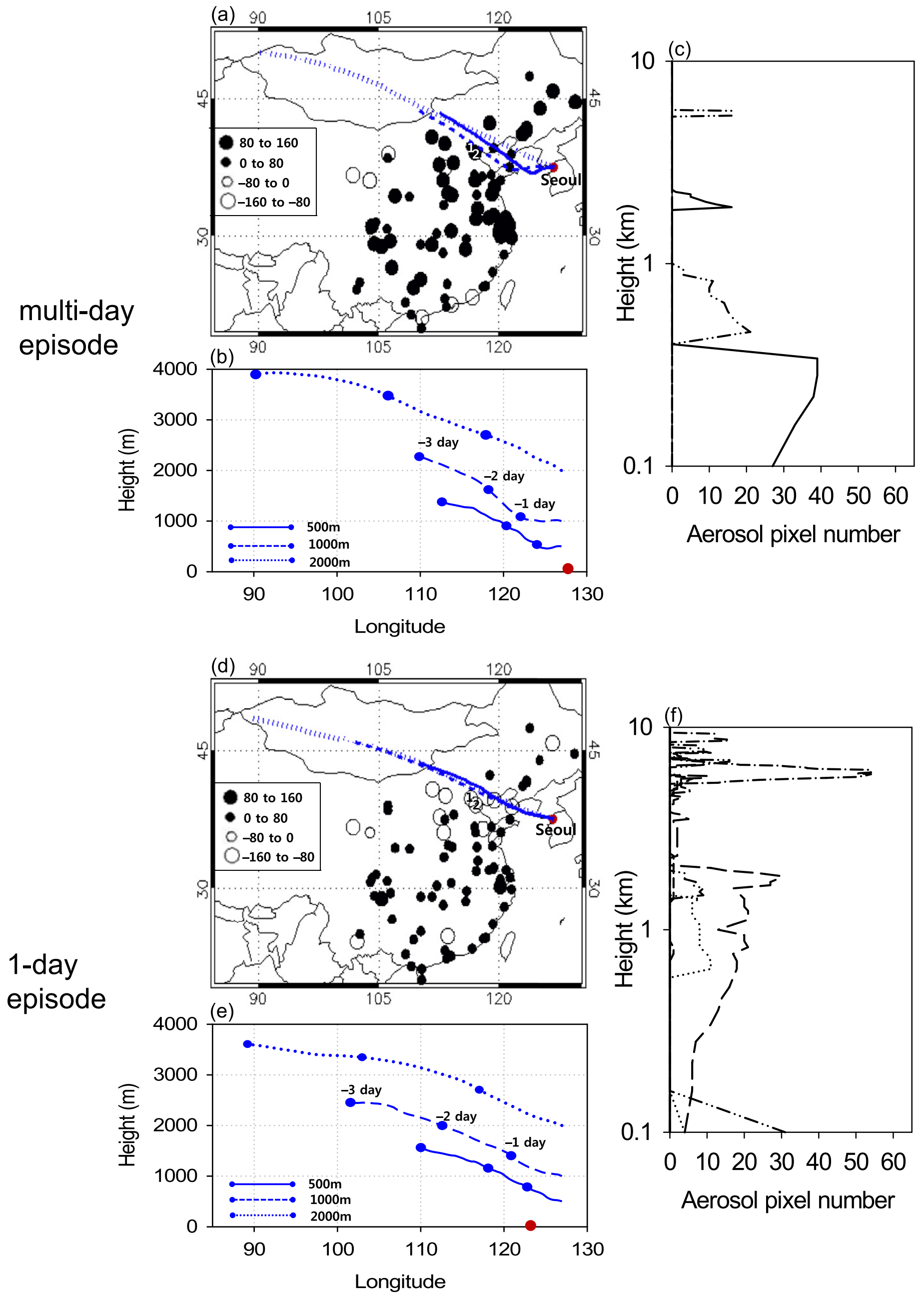

Fig. 6. Spatial distribution (a and d) of anomalous PM_{10} concentrations measured from each of the 83 sites on −1 day of high-PM10 episodes, and 72-h wind back trajectory from the HYSPLIT model (a, b and d, e). The circle size in each figure denotes the anomalous PM_{10} concentration against monthly climatology, respectively. The stations in 1 and 2 in Fig. 3a and d are Beijing and Tianjin, respectively. Each closed circle is a 24 h interval in Fig. 3b and e. Vertical profile of aerosol pixel number for high-PM_{10} concentration episodes from the CALIOP. Each line denotes a collocated case around Seoul for multi-day (c) and 1-day (f) episodes.

atmospheric circulation over eastern China and Korea, as well as air pollutants emitted in northeast China, are closely related with multi-day high-PM_{10} episodes in Seoul. Based on these analyses, we established that the atmospheric fields over China and its neighboring countries may determine the amount of air pollutants transported from eastern China into Seoul, leading to the duration of high-PM_{10} episodes in Seoul. Compared to 1-day episodes, Seoul is found to be strongly affected by massive air pollution over eastern China in the early stage of a multi-day high-PM_{10} episode.

In this work, we have focused on the beginning of high-PM_{10} episodes in Seoul. However, it is considered that the process involved in the episodes and the end of multi-day episodes also need to be discussed. In this study, due to the lack of emission quantity data in Seoul, it was difficult to quantify the level of contribution from local emissions. Nevertheless, considering that multi-day episodes occur under a very strong anomalous high-pressure system with weak winds in Seoul, local emissions may further deteriorate the air quality in the metropolitan area. The large amount of PM_{10} during an episode eventually dissipates either through transport by westerlies or significant precipitation >0.5 mm (about 20% of the total episodes) via wet deposition (in 1-day episodes, wet deposition by precipitation accounted for approximately 23% of the total cases).

It is noted that the PM_{10} concentration in China and atmospheric circulations over the eastern China–Korea region in two days before the onset of a multi-day episode are closely related with the duration of high-PM_{10} episodes in Seoul (Figs. 4 and 5). The strong and widespread high pressure anomalies in the lower troposphere over the entire region of China help accumulate air pollutants in central and eastern China. As a result, PM_{10} concentration in eastern China begins to increase at 3 days before the onset of the high-PM_{10} episode and reaches its peak a day before its occurrence day. Besides, strong anomalous low pressure over the East Sea and the Okhotsk Sea stretching to the east of the Korean Peninsula acts as atmospheric blocking to maintain the multi-day high-PM_{10} episodes. Consequently, these favorable atmospheric circulations play a key role in intensifying the influence of China-originated air pollutants on high-PM_{10} episodes in Seoul. These precursors may be used to deliver advance warnings of multi-day high-PM_{10} episodes, as well as to enable air quality management in China to prevent future catastrophic air quality episodes in the interior and exterior of the country.

Acknowledgments

This work was funded by the Korea Ministry of Environment as 'Climate Change Correspondence R&D Program'. Yong-Sang Choi was supported by the Korean Ministry of Environment as part of the Eco-Innovation Project. The funders had no role in the study design, data collection and analysis, decision to publish, or presentation of the manuscript. The authors wish to thank for Mrs. Chun Hee Jeoung for her assistance in data handling at the initial stages of our work. The authors are appreciative of helpful comments by two reviewers.

References

Brook, R.D., Franklin, B., Cascio, W., Hong, Y., Howard, G., Lipsett, M., Luepker, R., Mittleman, M., Samet, J., Smith, S.C., Tager, I., 2004. Air pollution and cardiovascular disease: a statement for healthcare professionals from the expert panel on population and prevention science of the American Heart Association. Circulation 109, 2655–2671.

Chang, C.T., Tsai, C.J., 2003. A model for the relative humidity effect on the readings of the PM-10 beta-gauge monitor. J. Aerosol Sci. 34, 1685–1697.

Chen, B., Kan, H., 2008. Air pollution and population health: a global challenge. Environ. Health Prev. Med. 13, 94–101.

Chen, Z.H., Cheng, S.Y., Li, J.B., Guo, X.R., Wang, H.Y., Chen, D.S., 2008. Relationship between atmospheric pollution processes and synoptic pressure patterns in northern China. Atmos. Environ. 42, 6078–6087.

Draxler, R., Rolph, G., 2013. HYSPLIT (HYbrid Single-particle Lagrangian Integrated Trajectory) Model Access via NOAA ARL READY. NOAA Air Resources Laboratory, Silver Spring, MD. Available at: http://ready.arl.noaa.gov/HYSPLIT.php.

Fajersztajn, L., Veras, M., Barrozo, L.V., Saldiva, P., 2013. Air pollution: a potentially modifiable risk factor for lung cancer. Nat. Rev. Cancer 13, 674–678.

Fu, X., Wang, S.X., Cheng, Z., Xing, J., Zhao, B., Wang, J.D., Hao, J.M., 2014. Source, transport and impacts of a heavy dust event in the Yangtze River delta, China in 2011. Atmos. Chem. Phys. 14, 1239–1254.

Gold, D.R., Samet, J.M., 2013. Air pollution, climate, and heart disease. Circulation 128, 411–414.

Heo, J.B., Hopke, P.K., Yi, S.M., 2009. Source apportionment of $PM_{2.5}$ in Seoul, Korea. Atmos. Chem. Phys. 9, 4957–4971.

Jung, C.H., Cho, Y.S., Hwang, S.M., Jung, Y.G., Ryu, J.C., Shin, D.S., 2007. Analysis of measurement error for PM-10 mass concentration by inter-comparison study. J. Korean Soc. Atmos. Environ. 23, 689–698.

Kalnay, E., Kanamitsu, M., Kistler, R., Collins, W., Deaven, D., Gandin, L., Iredell, M., Saha, S., White, G., Woollen, J., Zhu, Y., Chelliah, M., Ebisuzaki, W., Higgins, W., Janowiak, J., Mo, K.C., Ropelewski, C., Wang, J., Leetmaa, A., Reynolds, R., Jenne, R., Joseph, D., 1996. The NCEP/NCAR 40-year reanalysis project. Bull. Am. Meteorol. Soc. 77, 437–471.

Korean Statistical Information Service. 2013. Available at: http://kosis.kr/wnsearch/totalSearch.jsp.

Lee, S., Ho, C.-H., Choi, Y.-S., 2011. High-PM10 concentration episodes in Seoul, Korea: background sources and related meteorological conditions. Atmos. Environ. 45, 7240–7247.

Lee, S., Ho, C.-H., Lee, Y.G., Choi, H.-J., Song, C.-K., 2013. Influence of transboundary air pollutants from China on the high-PM10 episode in Seoul, Korea for the period October 16–20, 2008. Atmos. Environ. 77, 430–439.

Lewandowska, A.U., Falkowska, L.M., 2013. High concentration episodes of PM_{10} in the air over the urbanized coastal zone of the Baltic Sea (Gdynia-Poland). Atmos. Res. 120, 55–67.

Lin, J., Pan, D., Davis, S.J., Zhang, Q., He, K., Wang, C., Streets, D.G., Wuebbles, D.J., Guan, D., 2014. China's international trade and air pollution in the United States. Proc. Natl. Acad. Sci. 111, 1736–1741.

Liu, Y.J., Zhang, T.T., Liu, Q.Y., Zhang, R.J., Sun, Z.Q., Zhang, M.G., 2014. Seasonal variation of physical and chemical properties in TSP, PM_{10} and $PM_{2.5}$ at a roadside site in Beijing and their influence on atmospheric visibility. Aerosol Air Qual. Res. 14, 954–969.

Nakajima, T., Yoon, S.-C., Ramanathan, V., Shi, G.Y., Takemura, T., Higurashi, A., Takamura, T., Aoki, K., Sohn, B.-J., Kim, S.-W., Tsuruta, H., Sugimoto, N., Shimizu, A., Tanimoto, H., Sawa, Y., Lin, N.-H., Lee, C.-T., Goto, D., Schutgens, N., 2007. Overview of the atmospheric brown cloud East Asian regional experiment 2005 and a study of the aerosol direct radiative forcing in east Asia. J. Geophys. Res. 112, D24S91.

OECD, 2012. Environmental Outlook to 2050: the Consequences of Inaction. The Organisation for Economic Co-operation and Development, p. 1. Available at: http://www.oecd.org/environment/oecdenvironmentaloutlookto2050theconsequencesofinaction.htm.

OECD, 2013. Regional Population Density: Asia and Oceania, 2012: Inhabitants Per Square Kilometre, TL3 Regions, vol. 2013. OECD Regions at a Glance.

Omar, A.H., Winker, D.M., Kittaka, C., Vaughan, M.A., Liu, Z., Hu, Y., Trepte, C.R., Rogers, R.R., Ferrare, R.A., Lee, K.P., Kuehn, R., Hostetler, C.A., 2009. The CALIPSO automated aerosol classification and lidar ratio selection algorithm. J. Atmos. Ocean. Technol. 26, 1994–2014.

Park, S.U., Cho, J.H., Park, M.S., 2013. Analyses of high aerosol concentration events (dense haze/mist) occurred in East Asia during 10–16 January 2013 using the data simulated by the aerosol modeling system. Int. J. Chem. 2, 10–26.

Qu, W.J., Arimoto, R., Zhang, X.Y., Zhao, C.H., Wang, Y.Q., Sheng, L.F., 2010. Spatial distribution and interannual variation of surface PM_{10} concentrations over eighty-six Chinese cities. Atmos. Chem. Phys. 10, 5641–5662.

Shen, G.F., Yuan, S.Y., Xie, Y.N., Xia, S.J., Li, L., Yao, Y.K., Qiao, Y.Z., Zhang, J., Zhao, Q.Y., Ding, A.J., Li, B., Wu, H.S., 2014. Ambient levels and temporal variations of $PM_{2.5}$ and PM_{10} at a residential site in the mega-city, Nanjing, in the western Yangtze River delta, China. J. Environ. Sci. Health Part A 49, 171–178.

Wang, F., Chen, D.S., Cheng, S.Y., Li, J.B., Li, M.J., Ren, Z.H., 2010. Identification of regional atmospheric PM_{10} transport pathways using HYSPLIT, MM5-CMAQ and synoptic pressure pattern analysis. Environ. Model. Softw. 25, 927–934.

Wang, K.C., Dickinson, R.E., Su, L., Trenberth, K.E., 2012. Contrasting trends of mass and optical properties of aerosols over the Northern Hemisphere from 1992 to 2011. Atmos. Chem. Phys. 12, 9387–9398.

Wang, L.T., Wei, Z., Yang, J., Zhang, Y., Zhang, F.F., Su, J., Meng, C.C., Zhang, Q., 2014. The 2013 severe haze over the southern Hebei, China: model evaluation, source apportionment, and policy implications. Atmos. Chem. Phys. 14, 3151–3173.

Winker, D.M., Tackett, J.L., Getzewich, B.J., Liu, Z., Vaughan, M.A., Rogers, R.R., 2013. The global 3-D distribution of tropospheric aerosols as characterized by CALIOP. Atmos. Chem. Phys. 13, 3345–3361.

World Meteorological Organization (WMO)/IGAC, 2012. Impacts of megacities on air pollution and climate. Available at: http://www.wmo.int/pages/prog/arep/gaw/gaw-reports.html.

World Health Organization (WHO), 2005. WHO Air Quality Guidelines for Particulate Matter, Ozone, Nitrogen Dioxide and Sulfur Dioxide. Global Update. Summary of Risk Assessment. Author, Geneva, Switzerland, pp. 9–13.

Yasunari, T., Taniguchi, M., Niles, D., Chen, D., 2013. Asia: proving ground for global sustainability. Curr. Opin. Environ. Sustain. 5, 288–292.

Zhang, R.J., Cao, J.J., Lee, S.C., Shen, Z.X., Ho, K.F., 2007. Carbonaceous aerosols in PM_{10} and pollution gases in winter in Beijing. J. Environ. Sci. 19, 564–571.

Zhang, X.Y., Gong, S.L., Shen, Z.X., Mei, F.M., Xi, X.X., Liu, L.C., Zhou, Z.J., Wang, D., Wang, Y.Q., Cheng, Y., 2003. Characterization of soil dust aerosol in China and its transport and distribution during 2001 ACE-Asia: 1. Network observations. J. Geophys. Res. 108, 1984–2012.

Zhang, W., Qian, C.N., Zeng, Y.X., 2014. Air pollution: a smoking gun for cancer. Chin. J. Cancer 33, 173–175.

Zhu, L., Huang, X., Shi, H., Cai, X., Song, Y., 2011. Transport pathways and potential sources of PM_{10} in Beijing. Atmos. Environ. 45, 594–604.